Effects of Curvature on the Initial Mixing Region of a Two-Dimensional Jet

Wataru Masuda* and Shigeo Andoh†
Technological University of Nagaoka, Japan

Results of hot-wire measurements in an initial mixing region of a two-dimensional curved jet are presented. It is found that the profiles of the rms intensity for the axial fluctuating velocity component and the Reynolds stress exhibit an obvious asymmetry due to the influence of the centrifugal force. By using the measured distribution of the mean velocities and the Reynolds stresses, the curvature factor and the eddy viscosity, which is included in the expression given by Sawyer, are estimated along the jet centerline, and it is shown that the Sawyer's expression is somewhat inadequate in the initial mixing region of a two-dimensional curved jet. The profiles of the terms in the turbulent energy equation and the Reynolds stress transport equation also exhibit an obvious asymmetry. However, the generation term and the pressure-strain redistribution term in the Reynolds transport equation exhibit an obvious asymmetry only within the region of about a few slot thicknesses downstream of the nozzle exit, and the asymmetry of these terms decays very rapidly.

Nomenclature

b_0	= slot thickness
$b_{1/2}$	= jet-half thickness
C	= curvature factor
L	= thickness of the shear layer
p	= fluctuation in the static pressure
R	= radius of curvature of the jet centerline
t	= time
U,V,W	= mean velocity components in the x, y, and z directions
u,v,w	= fluctuating velocity components in the x, y, and z directions
U_c	= velocity at the jet centerline
U_0	= velocity at the nozzle exit
x,y,z	= coordinate system
ϵ	= dissipation term
ν	= kinematic viscosity
ν_T	= eddy viscosity
ρ	= density
τ	= Reynolds stress

Introduction

CURVED jets have been used in some engineering applications. Recently, the development of aerodynamic windows,[1,2] in which one or more curved jets are used, is a subject that has received increasing attention. In high-power gas lasers, the extraction of a laser beam from a cavity through a solid window is difficult, since the heating caused by the absorption of laser energy may distort the window. Instead of solid materials, an aerodynamic window makes use of one or more two-dimensional gas jets to permit the extraction of a laser beam and support the pressure difference between the lasing gas and atmosphere. Due to the presence of the constant pressure difference, the two-dimensional jets bend along a circular arc. Therefore, the coherence of the laser beam extracted through the aerodynamic window is degraded by the turbulent structure of the curved jets. In order to predict precisely the optical characteristics of the extracted laser beam, the understanding of the turbulent structure of the curved jet along a circular arc is indispensable.[3,4]

Received Oct. 9, 1987; revision received Feb. 19, 1988.

*Associate Professor, Department of Mechanical Engineering.
†Graduate Student, Department of Mechanical Engineering.

The two-dimensional straight jet has been investigated extensively, and sufficient data on it are available for many practical engineering purposes. The authors also have reported the hot-wire measurements for an initial mixing region of a plane turbulent jet.[5] For curved jets, Prandtl suggested that there should be an enhanced mixing in the outer portion of the curved jet and reduced mixing in the inner portion of it due to the influence of centrifugal forces on the parcels of fluid, which transfer momentum from layer to layer. Since then, the curvature effects have been studied experimentally and theoretically, mostly on the turbulent wall-shear layers. However, there have been very few studies[6,7] of the turbulent free-shear layers. It should be pointed out that no author has treated the curvature effects on the initial mixing region of the two-dimensional jet. In the present investigation, therefore, the structure of the initial mixing region of a two dimensional curved jet along a circular arc is measured by hot-wire probes. The measurements include mean velocity, turbulent intensities, turbulent shear stress, terms in the turbulent energy equation, and terms in the Reynolds stress transport equation.

Experimental Apparatus and Procedure

The apparatus used in the present investigation is shown schematically in Fig. 1. The apparatus consists of a two-dimensional nozzle, cubic test chamber, and exhaust opening. A blow-down air supply system is used to provide the airflow to the nozzle, whose exit thickness b_0 and aspect ratio are 10 and 20 mm, respectively. Before reaching the nozzle, the air passes through a settling chamber, which contains screens to produce a uniform velocity at the nozzle exit. The contraction section of the nozzle consists of two arcs with the radius of 29 mm and is followed by a constant area section of 40 mm in length. The jet generated by the nozzle is injected into the test chamber and is exhausted through an opening downstream of the test chamber. The width of the exhaust opening is 50 mm. As shown in Fig. 1, the nozzle exit plane is inclined to the upstream wall of the test chamber with an angle of 30 deg. Therefore, a curved jet confined by the two vertical walls of the test chamber is generated automatically by injecting air into the test chamber continuously. The experiments are carried out with the slot Reynolds number set at 1.7×10^4. At the nozzle exit, the displacement thickness and momentum thickness of the nozzle wall boundary layers calculated from the measured velocity profiles are about 0.15 and 0.08 mm, respectively, and the measured turbulence level is 0.65%. The curved jet confined by two vertical walls of the test chamber is two-dimensional except in the vicinity of the walls. The variations in the mean velocity

and turbulence level across the span do not exceed 1% over 90% of the span width even at a downstream distance of 20 b_0.

In the present experiments, part of the curved jet necessarily impinges on the downstream wall near the exhaust opening.[7] Therefore, the impingement process might have some effects on the upstream mechanics of the jet. However, the reattaching jets and jets used in air cushion vehicles, which are the typical curved jets along a circular arc, also necessarily impinge on the downstream wall very strongly, and there is at least one narrow recirculating region on the jet boundaries. In the turbulence measurements of a curved jet along a circular arc, it is impossible to exclude these effects completely from the curvature effects. However, even in the case of the reattaching jet flows,[8] it is believed that the effects of the impingement process on the upstream mechanics of the jet are mostly restricted within the near field of the reattachment point. In the present experiments, it is expected that the influence of the exhaust opening on the initial mixing region of the curved jet is very weak, since the impingement is weak and the regions on the jet boundaries are large compared to the reattaching jets. It is also pointed out that there is no flapping motion of the jet in the present experiments.

The coordinate system used in the present paper is also shown in Fig. 1, where x is the coordinate parallel to the jet centerline and y and z are the coordinates perpendicular to the jet centerline. In the present paper, the jet centerline is defined as the streamline issuing from the center of the nozzle exit. In order to determine the jet centerline, an electrically heated tungsten wire of 0.2 mm diam can be fixed at the center of the nozzle exit along a spanwise line. Then, the path of the streamline starting at the wire is traced by traversing a thermocouple normal to the heated wake. The velocity is measured by setting the axis of the probe parallel to the jet centerline.

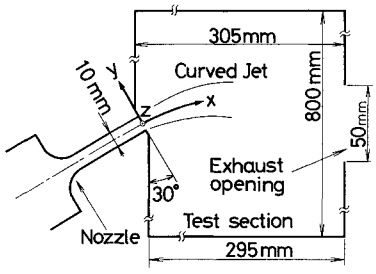

Fig. 1 Experimental apparatus.

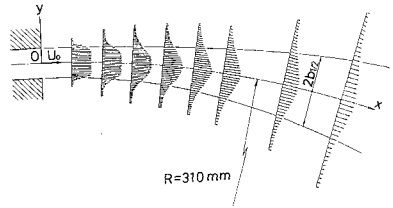

Fig. 2 Mean velocity profiles in the flowfield.

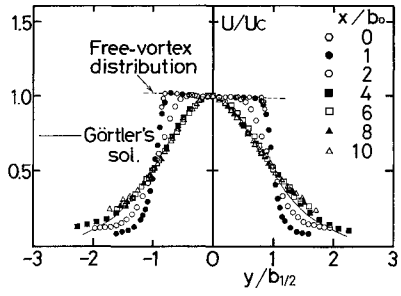

Fig. 3 Mean velocity profile.

Measurements of the mean velocity components U, V, and W and the fluctuating velocity components u, v, and w in the x, y, and z directions, respectively, are performed using X-wire and single-wire probes along with constant temperature anemometers and linearizers. These wires are constructed from 5 μm platinum-coated tungsten wire with an active length of 1 mm. The distance between the two wires of the X-wire probes is of the order of one wire length. The probe is calibrated before and after each run to check for the repeatability of the calibration. When X probes are used, the simple cosine law is used to decompose the velocities. The X-wire probes can be used in oblique operation for measuring velocity components with adequate accuracy up to an angle of 25 deg. The signals are registered in a data recorder, digitalized, then processed by a microcomputer. The dissipation term in the turbulent energy equation is evaluated by an analog differentiator. All components are calibrated for frequencies ranging from dc to 10 kHz. A split film probe,[7] whose diameter and active length are 152 μm and 2 mm, respectively, is also used in some measurements. However, only measured results obtained by the X-wire probe are given in the present paper, since the turbulent intensities and Reynolds stress obtained by the X-wire probe and the split film probe agree with each other within an error of approximately 5%.

Results and Discussion

Figure 2 shows the mean velocity profiles along the jet centerline measured by the electrically heated tungsten wire and the thermocouple. The momentums of the outer ($y>0$) and inner ($y<0$) portions of the jet centerline agree with each other within an error of 3%. Therefore, the jet centerline is determined very accurately. As shown in Fig. 2, the jet centerline is almost circular and its radius obtained by the least-squares method is 310 mm. The profiles of the mean velocity U normalized with respect to the velocity at the jet centerline U_c are shown in Fig. 3, where $b_{1/2}$ is the jet half-thickness. It is seen that the velocity profile at the nozzle exit agrees very well with the free-vortex distribution except in the outer and inner shear layers, since the inviscid flowfield is irrotational and the streamlines are circular. The potential core becomes thin as the shear layers develop and disappears about four slot thicknesses downstream of the nozzle exit. The velocity profile is almost similar beyond $x/b_0>4$ and agrees very well with the Görtler profile.

The growth of the shear-layer thickness L and jet half-thickness $b_{1/2}$ with downstream distance is presented in Fig. 4 and compared with the previous result about a straight jet.[5] The superscripts + and − in Fig. 4 represent the outer and inner portion of the curved jet, respectively. In the present paper, the definition of L is as follows:

$$L = U_c/\left(\frac{\partial U}{\partial y}\right)_{\max} \tag{1}$$

It is seen from Fig. 4 that L^+ is somewhat larger than L^- in the initial mixing region of the curved jet due to the influence of the centrifugal force. However, the difference betwen L^+ and L^- decreases in the downstream direction. Sawyer[8] also showed in the self-preserving state that the mean velocity

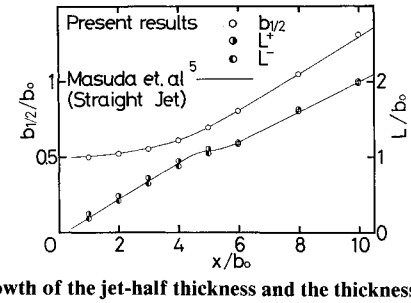

Fig. 4 Growth of the jet-half thickness and the thickness of the shear layers.

profile of a curved jet is almost symmetric in spite of the different entrainment rates on two sides of the jet and pointed out that this results from the presence of a flow across the jet. Figure 4 shows that $b_{1/2}$ and L of the curved jet agree very well with those of the straight jet. Therefore, it is expected that the influence of the impingement process and the boundary conditions on the initial mixing region of the curved jet is very weak.

The centerline axial velocity distribution is shown in Fig. 5 together with the results for a straight jet[5] given for comparison. Figure 5 also shows that the effect of curvature on the decay of the mean velocity is not significant. The present result also confirms that the effects of exhaust opening on the initial mixing region are very weak.

The conventional rms values of the fluctuating velocity components u, v, and w are shown in Fig. 6, whereas the Reynolds stress is shown in Fig. 7 and compared with the results for a straight jet given by Gutmark.[9] Gutmark's results were obtained far downstream from the nozzle ($x/b_0 \doteqdot 100$), where velocity fluctuations have attained their self-preserving state. As shown in Fig. 6, the intensity profile of the rms value of u exhibits an obvious asymmetry due to the influence of the centrifugal forces on the parcels of fluid that transfer momentum from layer to layer. The turbulent intensity is clearly enhanced in the outer portion of the curved jet and reduced in the inner portion. On the other hand, the asymmetry in the rms values of v and w is weak compared to that of u. These results seem very reasonable, since the effect of the centrifugal force is not induced by the velocity components in the y and z directions.

The measured distribution of the Reynolds stress shown in Fig. 7 also exhibits an obvious asymmetry due to the influence of the centrifugal force. The Reynolds stress in the curved jet was given theoretically by Sawyer[8] as follows:

$$\tau = \rho \nu_T \left[\left(\frac{\partial U}{\partial y} \right) - C \left(\frac{U}{R} \right) \right] \tag{2}$$

where τ is the Reynolds stress, ρ the density, ν_T the eddy viscosity, and C the curvature factor. Sawyer[8] showed from the measurements of the reattaching jet flow that the value of C averaged within the region of 20 slot thicknesses is 5.29–7.87. Endo[10] and Masuda et al.[7] showed that C takes large value (possibly more than 10) in the initial mixing region, decreases rapidly in the downstream direction, and takes a final value of 3 in the self-preserving region. In the present study, the values of ν_T and C are evaluated by substituting the data on the Reynolds stress and mean velocity into Eq. (2) and using the least-squares method. The dependence of C on x is shown in Fig. 8, where C^+, C^-, and $\bar{C}$ are the values of C evaluated by the data in the outer portion, inner portion, and both sides of the jet, respectively. It is seen that the present result agrees well with the previous works. However, C^- is considerably larger than C^+ in the initial mixing region. The value of $\bar{C}$ is nearly the average of them. The difference between C^+ and C^- decreases rapidly downstream of the initial mixing region. This result clearly shows that C depends strongly on y as well as on x in the initial mixing region. The dependence of ν_T on x is shown in Fig. 9, where ν_T^+, ν_T^-, and $\bar{\nu}_T$ are values of ν_T evaluated by the data in the outer portion, inner portion, and both sides of the jet. The eddy viscosity in a two-dimensional simple shear layer was given by Görtler as follows:

$$\nu_T = 0.0667 L U_c \frac{dL}{dx} \tag{3}$$

The eddy viscosity in the self-preserving region of a two-dimensional straight jet was also given by Görtler as follows:

$$\nu_T = 0.322 b_{1/2} U_c \frac{db_{1/2}}{dx} \tag{4}$$

The values of ν_T calculated by Eqs. (3) and (4) are also shown in Fig. 9. The measured eddy viscosity increases with x. In the initial mixing region, the measured values agree fairly well with the calculation by Eq. (3). Downstream of the initial mixing region, the measured values approach the calculation by Eq. (4). It is seen that ν_T^+ is larger than ν_T^- in the initial mixing region. The value of $\bar{\nu}_T$ is nearly the average of them. However, the difference between ν_T^+ and ν_T^- decreases downstream of the initial mixing region. This result shows that the profiles of ν_T

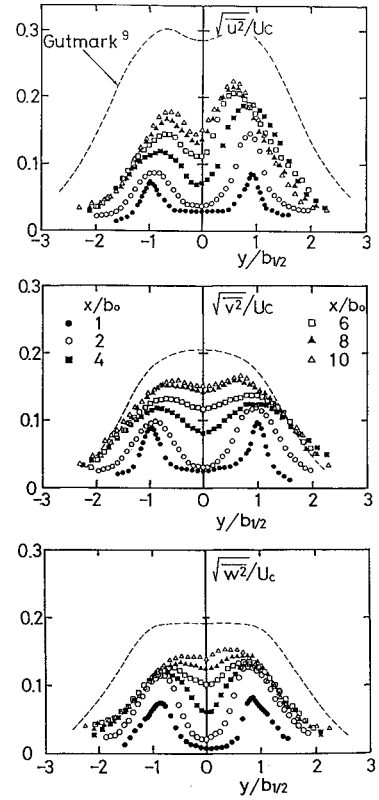

Fig. 6 Profiles of the rms intensity of the fluctuating velocity components u, v, and w.

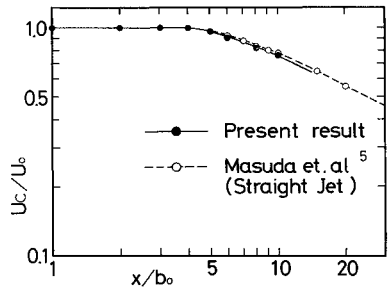

Fig. 5 Decay of the mean velocity along the jet centerline.

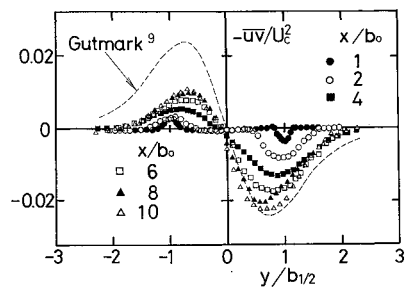

Fig. 7 Profiles of the Reynolds stresses.

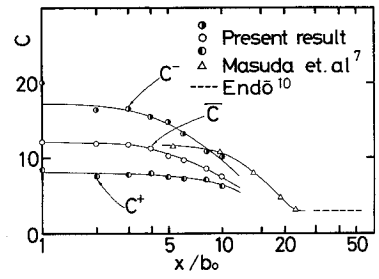

Fig. 8 Dependence of C on x.

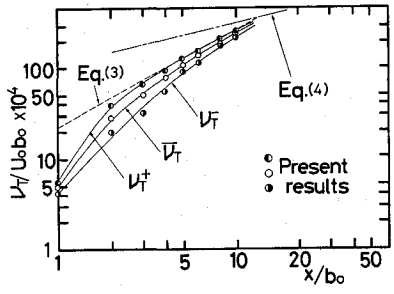

Fig. 9 Dependence of ν_T on x.

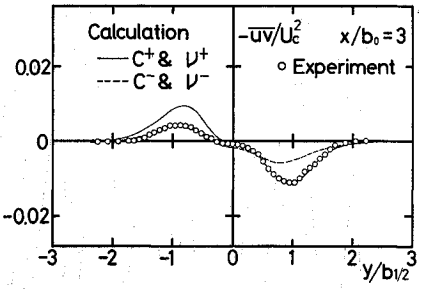

Fig. 10 Calculated profiles of the Reynolds stress using the mean velocity profile.

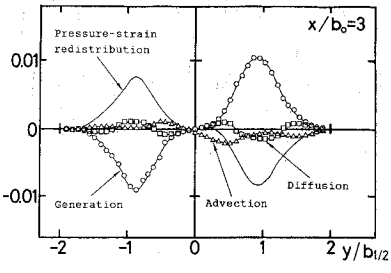

Fig. 11 Profiles of the terms in the Reynolds stress transport of Eq. (5).

are clearly asymmetric in the initial mixing region. In Fig. 10, the measured distribution of the Reynolds stress is compared with the distributions calculated from the mean velocity profile. One of the calculated results is obtained by using ν_T^+ and C^+, and the other by using ν_T^- and C^-. As a matter of course, the agreement between the measured and calculated distributions is excellent in the outer portion of the jet, provided ν_T^+ and C^+ are used. Similarly, excellent agreement is obtained in the inner portion of the jet, provided ν_T^- and C^- are used in the calculation. Equation (2) was proposed by Sawyer[8] in order to account for the effects of centrifugal forces on the Reynolds stress by introducing the curvature factor C. However, the profiles of ν_T obtained by the present experiments are clearly asymmetric in the initial mixing region. This means that the effects of the centrifugal forces cannot be eliminated completely from ν_T in spite of the introduction of C into Eq. (2).

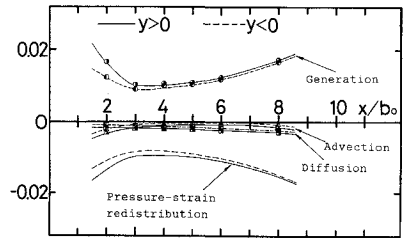

Fig. 12 Distributions of the peak values of the terms in the Reynolds stress transport of Eq. (5) along the jet centerline.

Therefore, Eq. (2) is somewhat inadequate to apply in the initial mixing region of a curved jet.

The equation representing the Reynolds stress transport in a two-dimensional curved jet is written in the form

$$\frac{R}{R+y}U\frac{\partial}{\partial x}\overline{(-uv)}+V\frac{\partial}{\partial y}\overline{(-uv)}-\frac{R}{R+y}\left(\frac{\partial V}{\partial x}-\frac{U}{R}\right)\overline{u^2}$$
$$-\overline{v^2}\frac{\partial U}{\partial y}+(\overline{u^2}-\overline{v^2})\frac{U}{R+y}+\overline{\frac{p}{\rho}\left(\frac{R}{R+y}\frac{\partial v}{\partial x}+\frac{\partial u}{\partial y}\right)}$$
$$-\frac{R}{R+y}\frac{\partial}{\partial x}\overline{\left[v\left(\frac{p}{\rho}+u^2\right)\right]}-\frac{\partial}{\partial y}\overline{\left[u\left(\frac{p}{\rho}+v^2\right)\right]}$$
$$-\frac{2\overline{uv^2}-\overline{u^3}}{R+y}=0 \qquad (5)$$

where p is the fluctuation in the static pressure. In Eq. (5), the first and second terms on the left represent advection; the third, fourth, and fifth terms, generation; the sixth term, pressure-strain redistribution; and the seventh, eighth, and ninth terms, diffusion. In the present investigation, the turbulent transport by pressure fluctuations is neglected, and the main destruction term in the Reynolds stress transport equation, the pressure-strain redistribution, is calculated using Eq. (5) and other measured terms to ensure the net Reynolds stress balance.[6] In Fig. 11 the profiles of the terms in the Reynolds stress transport equation are shown. The peak values of each term in the outer and inner portion of the jet are shown along the jet centerline in Fig. 12, where the signs of the values in the inner portion are changed. In Figs. 11 and 12, each term is made dimensionless by multiplying $b_{1/2}/U_c^3$. The profiles of the terms in the Reynolds stress transport equation exhibit an asymmetry due to the influence of the centrifugal force. Each term is enhanced in the outer shear layer of the curved jet and is reduced in the inner shear layer. In the Reynolds stress transport, the generation term and the pressure-strain redistribution term are the most significant. The absolute values of the peaks in the generation term and pressure-strain redistribution term decrease within the region $x/b_0<3$ and, thereafter, increase again in the downstream direction. The asymmetry in the profiles of these terms is strong near the nozzle exit. However, the asymmetry becomes weak in the downstream region. The main term in the generation is the fourth term in Eq. (5), which includes the turbulent intensity $\overline{v^2}$. It is thought that the weak asymmetry in the generation term is mostly due to the weak asymmetry of $\overline{v^2}$ as shown in Fig. 6.

The equation governing the balance of turbulent energy for the two-dimensional curved jet is written as follows:

$$\frac{R}{R+y}U\frac{\partial}{\partial x}\left(\frac{\overline{q^2}}{2}\right)+V\frac{\partial}{\partial y}\left(\frac{\overline{q^2}}{2}\right)+\frac{R}{R+y}(\overline{u^2}-\overline{v^2})$$
$$\times\left(\frac{\partial U}{\partial x}+\frac{V}{R}\right)+\overline{uv}\left(\frac{\partial U}{\partial x}-\frac{U}{R+y}+\frac{R}{R+y}\frac{\partial V}{\partial x}\right)$$
$$+\frac{R}{R+y}\frac{\partial}{\partial x}\overline{\left[u\left(\frac{p}{\rho}+\frac{q^2}{2}\right)\right]}+\frac{\partial}{\partial y}\overline{\left[v\left(\frac{p}{\rho}+\frac{q^2}{2}\right)\right]}$$
$$+\epsilon=0 \qquad (6)$$

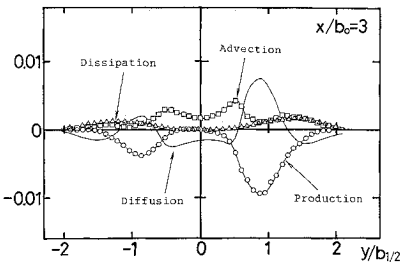

Fig. 13 Profile of the terms in the turbulent energy balance of Eq. (6).

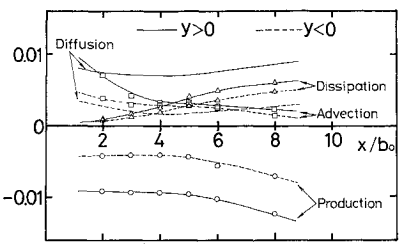

Fig. 14 Distributions of the peak values of the terms in the turbulent energy of Eq. (6) along the jet centerline.

where ϵ is the dissipation of turbulent energy and $q^2 = u^2 + v^2 + w^2$. The first and second terms of Eq. (6) represent advection; the third and fourth terms, production; the fifth and sixth terms, diffusion; and the seventh term, dissipation. The dissipation term ϵ is obtained by measuring the mean square of the time derivative of the u component of velocity and using the expression[11]

$$\epsilon = 15\nu\overline{\left(\frac{\partial u}{\partial t}\right)^2} \tag{7}$$

where ν is the kinematic viscosity and t the time. This expression assumes that the eddies primarily responsible for the dissipation are isotropic and move with the local mean velocity. In the present experiments, it is certain that wire-length effects lead to values of dissipation that are considerably small. Nevertheless, the energy balance is obtained by suitably scaling the measured value of viscous dissipation to ensure in the final energy balance that the net diffusion of the turbulent energy across the jet is zero.[11] The resulting energy balance is shown in Fig. 13. The peak values of each term in the outer and inner portion of the jet are shown along the jet centerline in Fig. 14. In Figs. 13 and 14, each term is made dimensionless by multiplying $b_{1/2}/U_c^3$. The main features of the energy balance are the following:

1) The profiles of the terms in the turbulent energy equation exhibit an obvious asymmetry. Each term is enhanced in the outer shear layer and reduced in the inner shear layer.

2) The advection term is large near the nozzle exit and decays rapidly within the initial mixing region.

3) The absolute value of the peak of the production term is nearly constant in the initial mixing region and, thereafter, increases in the downstream direction. The asymmetry in the profile of the production term is strong near the nozzle exit and it is preserved far downstream. The main term in the production is the fourth term in Eq. (6), where the Reynolds stress is included. It is thought that the strong asymmetry in the production term is due to the strong asymmetry of the Reynolds stress as shown in Fig. 7.

4) The asymmetry in the profile of the diffusion term is also strong near the nozzle exit, and it is preserved far downstream.

5) The dissipation term is very small near the nozzle exit. However, its magnitude and asymmetry grow in the downstream direction.

Conclusions

The following conclusions can be drawn from the experimental results about the initial mixing region of a two-dimensional curved jet along a circular arc.

1) The profiles of the rms intensity for the axial fluctuating velocity component and the Reynolds stress exhibit an obvious asymmetry due to the influence of the centrifugal force. On the other hand, the asymmetry in the rms intensity for the lateral fluctuating velocity components is weak.

2) The Sawyer's expression for the Reynolds stress is somewhat inadequate to apply in the initial mixing region of a curved jet, since the effects of centrifugal force cannot be eliminated completely from ν_T in spite of the introduction of the curvature factor.

3) The profiles of the terms in the Reynolds stress transport equation and turbulent energy equation also exhibit an asymmetry. However, the generation term and pressure-strain redistribution term in the Reynolds stress transport equation exhibit an obvious asymmetry only within the region of about a few slot thicknesses downstream of the nozzle exit, and the asymmetry of these terms decays very rapidly.

References

[1]Parmentier, E. M. and Greenberg, R. A., "Supersonic Flow Aerodynamic Windows for High-Power Lasers," *AIAA Journal,* Vol. 11, July 1973, pp. 943–949.

[2]Masuda, W., Maeda, Y., and Shirafuji, Y., "Subsonic Multiple-Jet Aerodynamic Window," *Review of Scientific Instruments,* Vol. 56, May 1985, pp. 677–681.

[3]Bogdanoff, D. W., "The Optical Quality of Shear Layers: Prediction and Improvement Thereof," *AIAA Journal,* Vol. 22, Jan. 1984, pp. 58–64.

[4]Sutton, G. W., "Fluctuation Intensity of Passive Species in a Turbulent Subsonic Jet," *AIAA Journal,* Vol. 7, Jan. 1969, pp. 90–95.

[5]Masuda, W. and Andoh, S., "Hot-Wire Measurements in an Initial Mixing Region of a Plane Jet," *Transactions of the Japan Society of Mechanical Engineers,* Vol. 497B, Jan. 1988, pp. 45–50 (in Japanese).

[6]Castro, I. P. and Bradshaw, P., "The Turbulence Structure of a Highly Curved Mixing Layer," *Journal of Fluid Mechanics,* Vol. 73, Pt. 2, 1976, pp. 265–305.

[7]Masuda, W. and Maeda, Y., "Measurements in a Two-Dimensional Curved Jet Along a Circular Arc," *Transactions of the Japan Society for Aeronautical and Space Sciences,* Vol. 29, Aug. 1986, pp. 67–76.

[8]Sawyer, R. A., "Two-Dimensional Reattaching Jet Flows Including the Effects of Curvature on Entrainment," *Journal of Fluid Mechanics,* Vol. 17, 1963, pp. 481–498.

[9]Gutmark, E. and Wygnanski, I., "The Planar Turbulent Jet," *Journal of Fluid Mechanics,* Vol. 73, Pt. 3, 1976, pp. 465–495.

[10]Endo, H., "Effects of Curvature on the Similar Structure and Turbulent Mixing of Two-Dimensional Curved Jets," National Aerospace Lab., Chofu, Japan, TR-156, 1968 (in Japanese).

[11]Bradbury, L. J. S., "The Structure of a Self-Preserving Turbulent Plane Jet," *Journal of Fluid Mechanics,* Vol. 23, Pt. 1, 1965, pp. 31–64.